JOURNAL OF MATERIALS SCIENCE 7 (1972) 1249–1259

A structural study of glassy polystyrene

S. M. WECKER, THEODORE DAVIDSON, J. B. COHEN
Department of Materials Science, The Technological Institute, Northwestern University, Evanston, Illinois, USA

X-ray scattering from three polystyrene glasses and from a partially devitrified specimen has been measured. The intensity data are identical for quenched and slowly cooled atactic polystyrene but differ for isotactic polystyrene quenched to the glassy state. Radial Distribution Functions (RDF) exhibit five principal peaks centred at 1.5, 2.5, 5, 6, and 10 Å for all of the glasses. A model RDF based on the published crystal structure is shown to compare well with the RDF obtained experimentally for devitrified isotactic polystyrene. On the basis of this model, peaks in the RDFs are assigned. It is shown that both inter- and intramolecular scattering contributes to the polystyrene RDF at distances beyond 3.7 Å. The structure is dominated by steric interaction of the phenyl groups, affecting both chain conformation and molecular packing.

1. Introduction

The tendency toward glass formation in linear polymers is most pronounced in those macromolecules which are atactic. Stereoregular syndiotactic and isotactic polymers can also be vitrified if cooled from the melt at such a rapid rate that crystallization does not intervene. It is known that variations in the conditions of vitrification or subsequent heat treatment affect the properties of polymer glasses [1-3]. The present study is a description of one high polymer glass, polystyrene, in terms of radial distribution functions calculated from X-ray scattering experiments.

X-ray studies on linear polymers date from the 1920s. Much of this early work has been discussed by Katz [4]. Most of it was concerned with positions of peaks in the pattern and their possible interpretation in terms of interchain and intrachain spacings. Katz pointed out the presence of an additional reflection in polystyrene which was not observed in styrene monomer. In 1936 Simard and Warren [5] obtained the radial distribution function (RDF) of unstretched natural rubber. This can be derived from X-ray measurements by Fourier transformation of suitably corrected intensity data. The RDF represents the density of atoms $\rho(r)$ in a spherical shell of thickness dr at a distance r from an "average" reference atom. This quantity consists of an average over the atoms in the irradiated volume of the sample and therefore represents the average structure of the sample. If more than one phase is present, the RDF obtained is a volume average of the RDF's of several phases. Simard and Warren found four peaks in their RDF out to 6Å and concluded that these were explicable in terms of the individual hydrocarbon chains in rubber and that no assumptions were necessary regarding the conformation or relative orientation of the chains.

Bjørnhaug, Ellefsen, and Tønnesen [6] applied this method in the early 1950s to several noncrystalline atactic polymers including polyvinylacetate, polymethylmethacrylate, and polystyrene. Their analyses show peaks at 1.5 and 2.5Å as is expected for polymers with carbon atoms in the chain backbone. These peaks correspond respectively to carbon atoms chemically bonded to nearest neighbours and to second nearest neighbours in a chain. These workers show a number of additional peaks in their RDFs out to 15Å. It appears from subsequent work, including this study, that some of these ripples are present as a result of truncation errors in the Fourier analysis.

In a study on atactic polystyrene, Krimm [7] observed two additional haloes centred at Bragg spacings of 8.84 and 4.67Å. For oriented samples of polystyrene, the scattering from the former

spacing was concentrated on the equator and that from the latter was toward the meridian. Krimm stated: "It appears that the 8.84Å peak arises from interference between atoms in neighbouring main chains, which are 9 to 10Å apart. The 4.67Å peak seems to be due to at least two different types of interatomic spacings: those between atoms in alternate phenyl groups in the same chain and those between atoms in phenyl groups and main chain atoms in neighbouring chains." On the basis of our analysis in Section 5 of this paper, there are a large number of different scatterers contributing to the third and higher peaks in the RDF. It appears that the earlier assignment [7] does not account for many of these contributions.

Kilian and Boueke [8] examined the scattering from glassy polystyrene at several temperatures and showed that the RDFs obtained were similar to those expected for model compounds as diverse as phenolphthalein and poly(*meta*-methylstyrene). This comparison indicated the importance of steric effects involving the bulky phenyl substituents on the macromolecules in determining chain conformation in the non-crystalline state. They showed that intramolecular effects dominate the diffraction pattern.

On a larger size scale than that examined in the present experiments, evidence of ordering in non-crystalline polymers has been suggested by observations in the electron microscope of a nodular structure on the order of 100Å in surface replicas of polysiloxanes [9], polystyrene [10], polyethylene terephthalate [11], and other polymers [12-14]. The origin and details of this fine structure have not been resolved.

Robertson [15] has shown that the actual densities of non-crystalline solid polymers are considerably greater than that predicted by a model for the random packing of chains.

This study is an attempt to obtain additional information on the structure of such non-crystalline polymers. The present study aims at more accurate RDFs than heretofore reported for polymers and areas of the peaks are reported and discussed. Polystyrene was chosen as a model material because it can be obtained in both crystalline and non-crystalline forms. The results of this study indicate that a short range structure exists in non-crystalline polystyrene caused by a tendency for phenyl rings to separate and chain segments to pack parallel to each other. As a result of these tendencies, there appear to be some differences in conformation in glassy atactic and isotactic polystyrene.

2. Experimental

2.1. Sample preparation

Three different samples were compression moulded from pellets into circular discs in a "picture frame" mould. Two of these samples, one atactic and one isotactic, were quenched into liquid nitrogen; the atactic sample from 205°C, the isotactic from 245°C. A third sample of atactic polystyrene was cooled at 1°C per minute from 205 to 70°C. All three of these glasses were optically transparent and showed no discrete X-ray scattering. After X-ray data was collected on these three non-crystalline samples, the isotactic sample was annealed at 178 ± 2°C for 12 h to obtain a partially devitrified semi-crystalline sample with density of 1.069 g cm^{-3}, compared to 1.056 g cm^{-3} for the as-quenched sample. Pertinent information on the different samples is summarized in Table I.

2.2. Data collection and analysis

X-ray measurements were made on a modified G.E. XRD-5 diffractometer [16]. The data for the non-crystalline samples were obtained with CuK_α radiation, using a doubly-bent lithium fluoride monochromator in the incident beam. Data were collected by point counting for a fixed number of counts (20000) at intervals of 0.25 degree from 6° 2θ, to 50° 2θ, and at intervals of 0.5 degree up to 150° 2θ. Measurements on the partially crystalline sample differed in that a graphite monochromator was used. In addition, the intervals in 2θ were 0.1° from 7.5° to 40° 2θ, 0.25° to 60° 2θ, and 0.5° to 140° 2θ; counting was for 100000 counts in a monitor counter. (The smallest number of detector counts was greater than 10000 in this mode.)

2.3. Corrections to experimental intensity

Before Fourier transformation, the data must be corrected for several experimental factors, which include background, polarization, absorption, and multiple scattering. Background was measured by placing a lead trap in the sample holder. The signal measured is the sum of electronic noise, air scatter, and cosmic radiation. Typical background values are 21% of the measured intensity at 6° 2θ, 3.5% at 15° 2θ, and 5% at 80° 2θ. The polarization correction is the standard correction for a monochromatic beam. If the receiving slits on a diffractometer allow the

TABLE I Description of the samples

Sample	114	115	118	118A
Tacticity	Atactic	Atactic	Isotactic* (15 to 20% atactic)	Isotactic (15 to 20% atactic)
Cooling rate	1°C/min	6°C/sec (at centre)	6°C/sec (at centre)	No. 118 annealed 18 h at 180°C
Density, g cm^{-3} ($\pm$ 0.0003)	1.048	1.048	1.056	1.069
Centre thickness, cm	0.5525	0.5715	0.5410	0.5610
$\bar{M}_n$	8.799×10^4	8.799×10^4	—	—
$\bar{M}_w$	2.983×10^5	2.983×10^5	5.7×10^5*	5.7×10^5*
Manufacturers designation	Styron 686	Styron 686	1140-16-1	1140-16-1

*Weight average molecular weight ($\bar{M}_w$) data for the isotactic samples was provided by Dr F. L. Saunders of the Dow Chemical Company. $\bar{M}_n$ (the number average molecular weight) and $\bar{M}_w$ for the atactic material were calculated from GPC data.

counter to "see" all the radiation diffracted by a flat faced sample, the absorption correction is a constant and need not be applied. However, if some radiation is blocked by the receiving slits because of deep penetration of the beam, the data must be multiplied by an absorption factor. This correction is given by Milberg [17]. Typical values for the absorption correction, in this experiment, are 0.115^{-1} at 6° 2θ, decreasing to 0.111^{-1} at 150° 2θ.

The data analysis assumes that detected radiation has been scattered only once in the sample. The ratio of doubly scattered to singly scattered radiation has been derived by Warren and Mozzi [18] for unpolarized incident radiation, and is of the form:

$$\frac{I(2)}{I(1)} \propto \frac{1}{\sum_i A_i \mu_i(m)} \qquad (1)$$

where A_i and $\mu_i(m)$ are the atomic weights and mass absorption coefficients of the atoms, and the summation is over a unit of composition. For heavy atoms, the summation is large and the correction can be ignored. For light atoms, this is not the case. If the incident radiation is polarized by a monochromator, a correction to Equation 1 is necessary. For the data collected using a LiF monochromator the correction to Equation 1 was applied; for the graphite monochromator ($\cos 2\theta_m = 0.894$) it was unnecessary [19]. $I(2)/I(1)$ was less than 2% at all points for all samples. After all corrections were applied, the data was extrapolated, "by eye", to 0° 2θ. The effect of neglecting small angle scattering can be estimated from the maximum possible density fluctuations that could occur on a scale measurable by small angle X-ray diffraction [20]. We have calculated that under the "worst possible" conditions this contribution to the results is 3% at $r = 10$Å (see [20] Equations 20 to 22). (For this calculation the differences in density of crystalline isotactic and amorphous atactic polystyrene were employed. The measured density was then used to obtain the amounts of the regions of these two densities.)

The precision of the X-ray data was determined by making three runs on each of the non-crystalline samples in the 8 to 28° 2θ region, point counting in 0.1° steps with the samples removed and replaced for each run. For a set of 1809 intensity measurements (made by running each of three samples three times) the average deviation from the mean intensity at any value of 2θ was less than 1%, for a given specimen.

3. The radial distribution function

The radial distribution function for a monatomic sample is derived from the X-ray data by Fourier Transformation:

$$rG(r) = 4\pi r^2[\rho(r) - \rho_0] = \frac{2r}{\pi}\int_0^\infty k\, I(k) \sin rk dk \qquad \ldots\ldots (2a)$$

$$I(k) = \left\{\frac{I}{f^2} - 1\right\} \qquad (2b)$$

where r is the radial distance from an arbitrary reference atom, $\rho(r)$ the atomic density at r, ρ_0 the average atomic density, $k = 4\pi \sin\theta/\lambda$, I is the experimental coherent intensity in electron units/atom, and f is the scattering factor for the atom. Before transformation, the corrected experimental data must be converted from the arbitrary scale of measurement to a scale of electron units per atom, and the incoherent contribution must be subtracted. The effect of errors introduced in these steps on the resulting

RDF, along with the effect of a finite limit on the integral over k ($k_{max} = 8.15$ with the Cu radiation employed in this study) and the correction of these errors has seen discussed by Kaplow, Strong, and Averbach [21]. The general principles of their methods are followed in this analysis.

Multiplication by a conversion constant α normalizes the intensity to electron units. A small error in α produces large oscillations in $G(r)$ at distances close to $r = 0$; α was chosen to minimize these oscillations. The smallest oscillations were obtained when α was found by solving the following equation [22]:

$$-2\pi\rho_0 Z^2 = \alpha \int_0^{k_{max}} I_{ex}\, k^2\, dk - \int_0^{k_{max}} k^2 (I_{inc} + f^2)\, dk \qquad (3)$$

where Z is the atomic number of the atom, I_{ex} is the experimental intensity in arbitrary units, I_{inc} is the incoherent scattering, and ρ_0 is determined by measuring the sample's macroscopic density.

Termination of the integration in Equation 2a at a value of k less than infinity introduces subsidiary maxima about the main peaks in $G(r)$ Spurious maxima in $G(r)$ are identifiable by their behaviour when $F(k)$ is intentionally truncated at several different values of k, and they are smoothed out of the $G(r)$ curves. $G(r)$ is then re-transformed to $F(k)$, but now only for k values greater than the measured k_{max}. The result is added to the experimentally determined $F(k)$. This process is iterated until no substantial changes in $G(r)$ occur.

Errors in scattering factors also produce large oscillations in the RDF at small distances. Values used in the present study were obtained from the works of McWeeny [23] for f_C, the scattering factor for carbon, Hanson [24] for f_H, the scattering factor for hydrogen, Keating and Vineyard [25] for the incoherent scattering factor for carbon $(I_{inc}/R)_C$, and Compton and Allison [26] for $(I_{inc}/R)_H$. R is the recoil factor.

The equations for scattering by a monatomic material were used in this case by defining a hypothetical scatterer with the properties: $f^2 = f_C^2 + f_H^2$, $I_{inc}/R = (I_{inc}/R)_C + (I_{inc}/R)_H$, and $Z^2 = Z_C^2 + Z_H^2$. The errors in these scattering factors are corrected by making use of the fact that for r less than the distance of closest approach for neighbouring atoms (r_0), $\rho(r) = 0$. In this region $4\pi r[\rho(r) - \rho_0]$, should be a straight line of slope $-4\pi\rho_0$. Defining functions

$$\Delta G(r) = -4\pi r\rho_0 - G(r)_{orig},$$

and

$$\Delta[kI(k)] = [kI(k)]_{corr} - [kI(k)]_{orig},$$

the error in $kI(k)$ can be determined by Fourier Transformation:

$$\Delta[kI(k)] = \int_0^{\infty} \Delta G(r) \sin kr\, d(r) \qquad (4)$$

Since $\Delta G(r)$ is only available up to approximately r_0, the upper limit of integration is considerably less than infinity, and several iterations of the correction procedure are necessary to eliminate the error. (By forcing the initial slope of the RDF to match the observed macroscopic density we lose the possibility of comparing the initial slope and measured density as Kaplow, Strong, and Averbach have done, but as mentioned earlier, the initial slope is sensitive to small angle scattering; as we did not measure this, this slope would not be corrected anyway.)

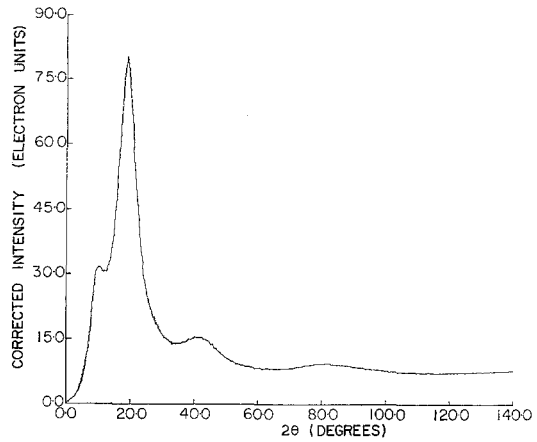

Figure 1 Diffraction pattern from quenched atactic polystyrene. The data was corrected for background, polarization, absorption, multiple scattering, and converted to electron units with Equation 1. Compton scattering has not been removed.

4. Results

4.1. Diffraction patterns

The diffraction pattern for quenched atactic polystyrene is shown in Fig. 1. The major features are broad peaks at 11, 19, 42 and 81 degrees 2θ.

Comparing the slowly cooled atactic to the quenched atactic, the data points for the two show an average deviation of 1.1%. This is essentially the statistical fluctuations in counting.

In essence, the diffraction data are the same for the slowly cooled atactic and quenched atactic samples. A slight shift of the first two haloes to lower angles, corresponding to larger spacings, is present in the diffraction pattern of quenched isotactic polystyrene (Fig. 2). This at first suggests more open packing and a lower density than the atactic material, yet the average density of the isotactic material is higher. This is discussed in Section 6 below.

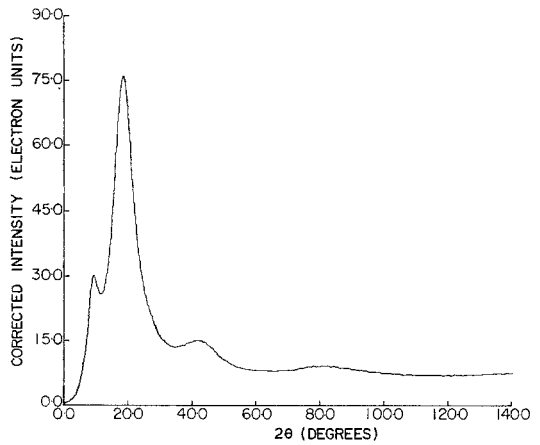

Figure 2 Diffraction pattern from quenched isotactic polystyrene.

The diffraction pattern of the annealed isotactic sample, shown in Fig. 3, consists of crystalline peaks superimposed on a non-crystalline background. The peaks seem to rise

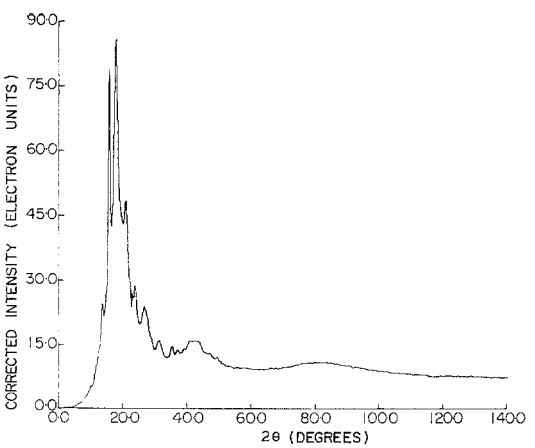

Figure 3 Diffraction pattern from annealed isotactic polystyrene.

out of the low angle side of the non-crystalline halos. Low diffraction angles correspond to large spacings in the sample and large spacings to low density, yet the partly crystalline sample is the most dense.

4.2. Radial distribution functions obtained for polystyrene

Fig. 4 compares the $G(r)$ for quenched and slowly cooled specimens of atactic polystyrene. That the squares representing $G(r)$ for the slowly cooled samples fit exactly on the line representing the quenched sample indicates the degree of similarity of their X-ray structure.

Fig. 5a compares $G(r)$ for quenched isotactic polystyrene to $G(r)$ for the quenched atactic material. The displacements between the squares and the line indicate the differences between these two specimens. Fig. 5b shows the segment of Fig. 5a from 4 to 16Å on an enlarged scale.

Fig. 6 shows $G(r)$ versus r for the isotactic sample partially crystallized by annealing. All samples show peaks in the vicinity of 1.5, 2.5, 5, 6, and 10Å. In addition, the non-crystalline samples have a peak at about 15Å. The positions and heights of these peaks are given in Table II. Peaks in $G(r)$ were measured at the centre of a line drawn horizontally through each peak at half its maximum height. The precision of this determination is estimated at $\pm$ 0.05Å. We now offer a plausible explanation based on the trends in these data, but it should be kept in mind that the similarities between RDFs are greater than the differences.

The first peak corresponds to the bonded nearest neighbour C-C distance. The peak position and height for all non-crystalline samples are close (1.5Å, 2.10 to 2.17 high). The partly crystalline sample has a higher and narrower 1.5Å peak than the other samples; the reason for this difference is not known. The number of atoms in the 0 to 2Å interval for all samples lies between 2.10 and 2.14 atoms, close to the theoretical value of 2.25. The values for each specimen (and theoretical values whose source is described in Section 4.3) are presented in Table III. The largest discrepancy between measured and predicted values is 7%.

The second peak corresponds to second nearest-neighbour bonded distances, with a few "cross phenyl ring" distances included at the upper end of the interval. The peak occurs at 2.5Å for all samples with peak height ranging from 1.54 to 1.72. The number of atoms in the

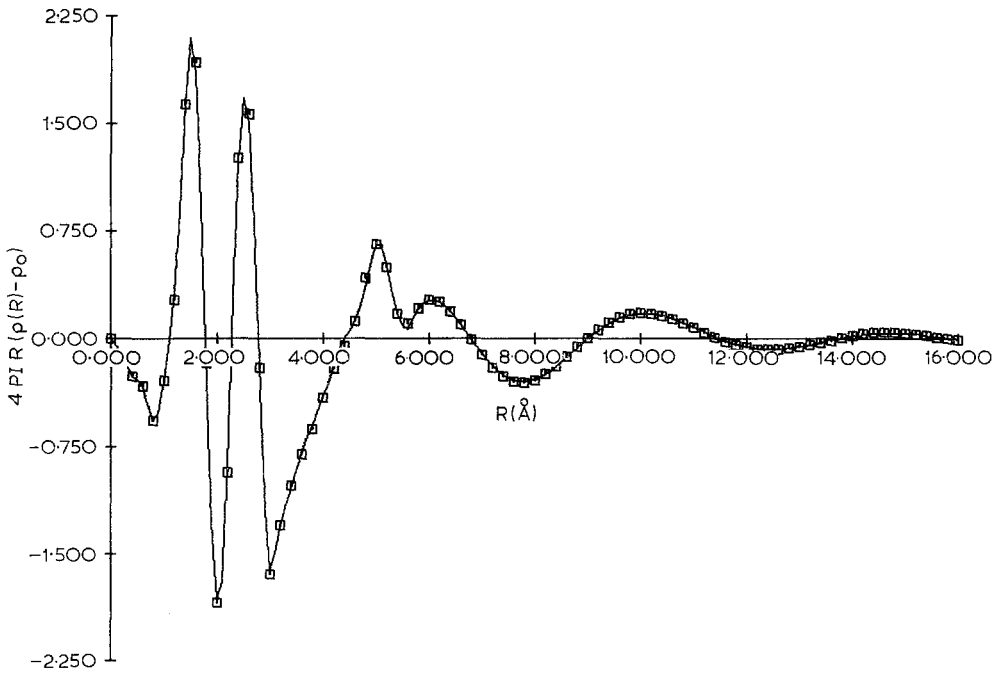

Figure 4 The squares are $G(r)$ versus r for slowly cooled atactic polystyrene. The line is $G(r)$ versus r for quenched atactic polystyrene. The two functions are seen to superimpose. This shows both the precision of the analysis and the identical nature of the two atactic materials with differing thermal histories.

2.3Å interval ranges from 3.87 to 4.23 (see Table III); the predicted value is 4.0.

The third peak at 5Å shifts to lower spacings and intensity with increasing perfection (quenched atactic to quenched isotactic to annealed isotactic). This is accompanied by a shift to higher spacings and intensity for the fourth peak at 6Å. Because of ambiguities in interpretation (see below), the number of atoms in intervals beyond 3Å was not calculated. The remaining peaks at 10 and 15Å show increases in spacing accompanied by decreases in intensity. (These shifts can be clearly seen by examining the $G(r)$'s in detail; they are most clearly delineated by examining the positions of an entire peak, not just its maximum, or any other single position.)

As a check on the reproducibility of the data

TABLE II Peaks in $G(r)$ and their heights

Polystyrene sample	Peak 1		Peak 2		Peak 3	
	Position	Height	Position	Height	Position	Height
Quenched atactic	1.51Å	2.10	2.53Å	1.68	5.05Å	0.657
Slowly cooled atactic	1.51	2.15	2.53	1.72	5.01	0.662
Quenched isotactic	1.51	2.17	2.53	1.72	5.00	0.654
Annealed isotactic	1.43	3.49	2.49	1.54	4.94	0.516
	Peak 4		Peak 5		Peak 6	
	Position	Height	Position	Height	Position	Height
Quenched atactic	6.11Å	0.265	10.1Å	0.175	14.7Å	0.0393
Slowly cooled atactic	6.09	0.267	10.0	0.180	14.6	0.0458
Quenched isotactic	6.13	0.285	10.3	0.140	14.9	0.0267
Annealed isotactic	6.42	0.351	10.7	0.100	—	—

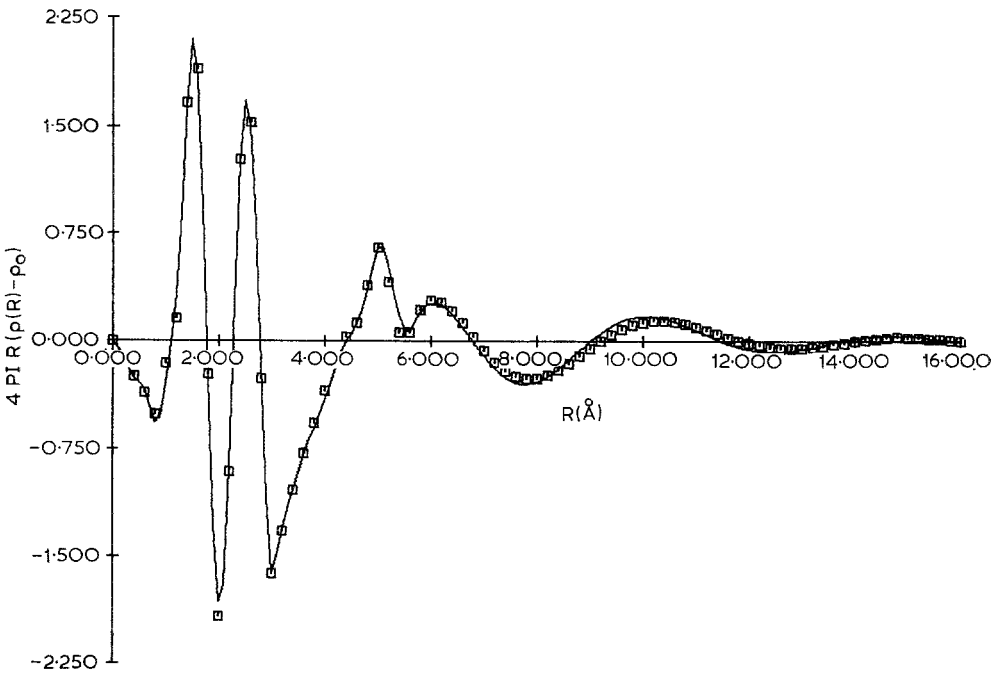

(a)

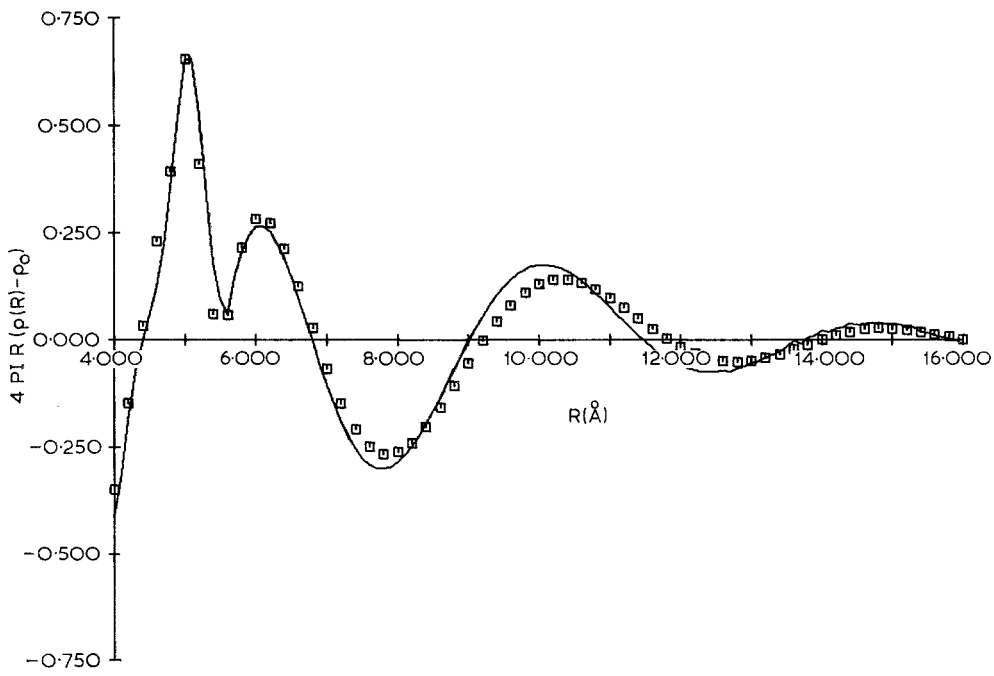

(b)

Figure 5 (a) The squares are $G(r)$ versus r for quenched isotactic polystyrene. The line is $G(r)$ versus r for quenched atactic polystyrene. The width of a square is 0.2Å; estimated independently, the precision of a position is $\pm$ 0.05Å (see text). (b) Enlargement of the 4 to 16Å region of Fig. 5a.

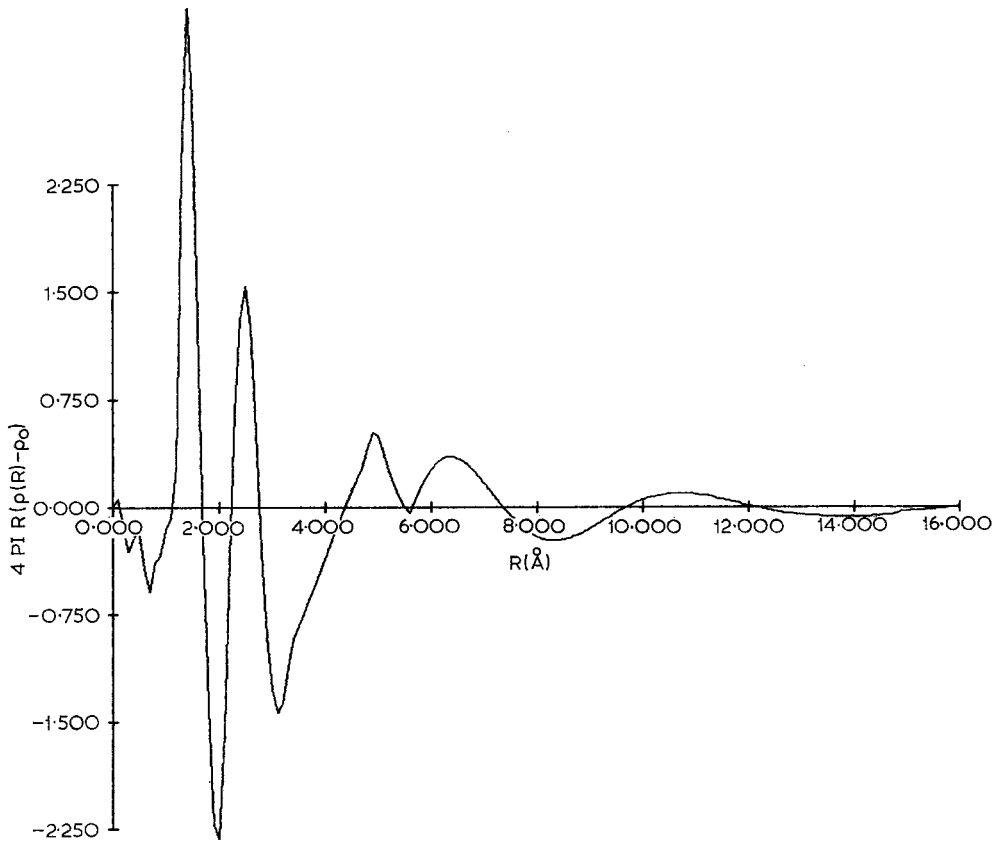

Figure 6 $G(r)$ for annealed isotactic polystyrene.

TABLE III Comparison of areas in various intervals of $G(r)$ versus predicted values

	Atoms in Interval	
Sample	0 to 2Å	2 to 3Å
Quenched atactic*	2.10	3.91
Slow cooled atactic*	2.15	3.89
Quenched isotactic	2.12	3.87
Annealed isotactic	2.14	4.23
Theoretical (from model)	2.25	4.0

*The diffraction patterns for these two specimens were essentially identical so that the differences between the values give an indication of the error in data processing.

analysis, $G(r)$ of the slowly cooled atactic sample was also calculated. Since the diffraction patterns of the quenched and slow-cooled samples are identical, as indicated earlier, their RDFs should also be identical (see Fig. 4). At their greatest separation, the $G(r)$ values for the two samples differ by 0.098 atoms $Å^{-2}$. The two atactic samples, differing in thermal history, have identical densities and have $G(r)$s which are identical within the precision of our results.

4.3. Model RDF

In attempting to analyse the peaks beyond 2.5Å, a "theoretical" $G(r)$ was calculated based on the crystal structure of isotactic polystyrene. Isotactic polystyrene crystallizes in a trigonal unit cell, space group $R3C$ or $R\bar{3}C$, with lattice parameters along the cell edge of 21.9Å, and along the chain direction of 6.65Å [27]. Diffraction introduces a centre of symmetry which necessitates using the $R\bar{3}C$ space group. A unit cell is shown in Fig. 7. Using the crystallographic data, the distances to all carbon atoms within 8Å of the carbon atoms in one repeat unit were computed. A repeat unit is defined as a phenyl ring and its adjoining "chain" atoms, of chemical composition—$CH_2CHC_6H_5$—, which is repeated to form the polymer chain. Since all repeat units in the unit cell lie on a rank eighteen equipoint,

the choice of reference repeat unit for the calculation has no effect on the final result.

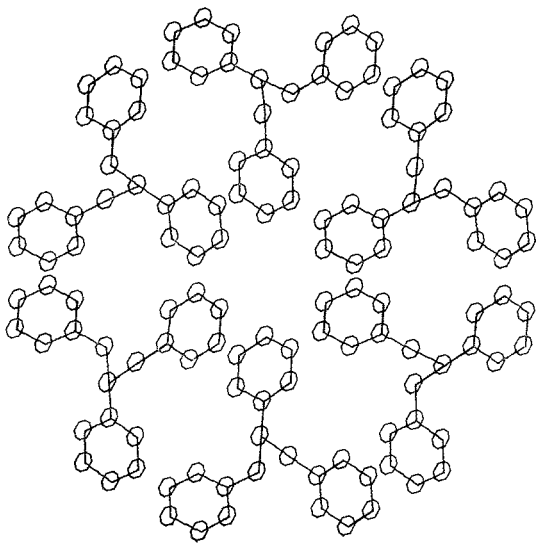

Figure 7 Unit cell of crystalline polystyrene, projected onto an (001) plane.

Eight $G(r)$'s were obtained using each atom in the repeat unit as the origin, and were averaged to obtain the final result, shown in Fig. 8. Theoretical values are given by the histogram; the smooth curve is the experimental $G(r)$ for the partially crystalline isotactic sample. The same computer program that was written to calculate the distribution of interatomic distances also produced a listing of all atom pairs separated by 8Å or less. This made possible an attempt at determining the location and identity of the atoms involved in a peak in $G(r)$.

5. Comparison of model and experiments

There is a great deal of similarity between the theoretical and experimental $G(r)$'s. Both have peaks at approximately 1.5 and 2.5Å, and a broad peak in the 6.5Å region. In place of the single peak at 5Å however, two peaks, at 3.7 and 4.7Å, exist in the theoretical curve.

The first peak contains 2.25 atoms and it is caused exclusively by bonded neighbours along the chain and in the phenyl rings. The second peak is caused by second nearest neighbours in the molecule, and some distances across the phenyl ring to third nearest neighbour atoms. It contains 3.75 atoms. (These are the theoretical values from the model and are summarized in Table III.) The third peak, centred at about 3.7Å,

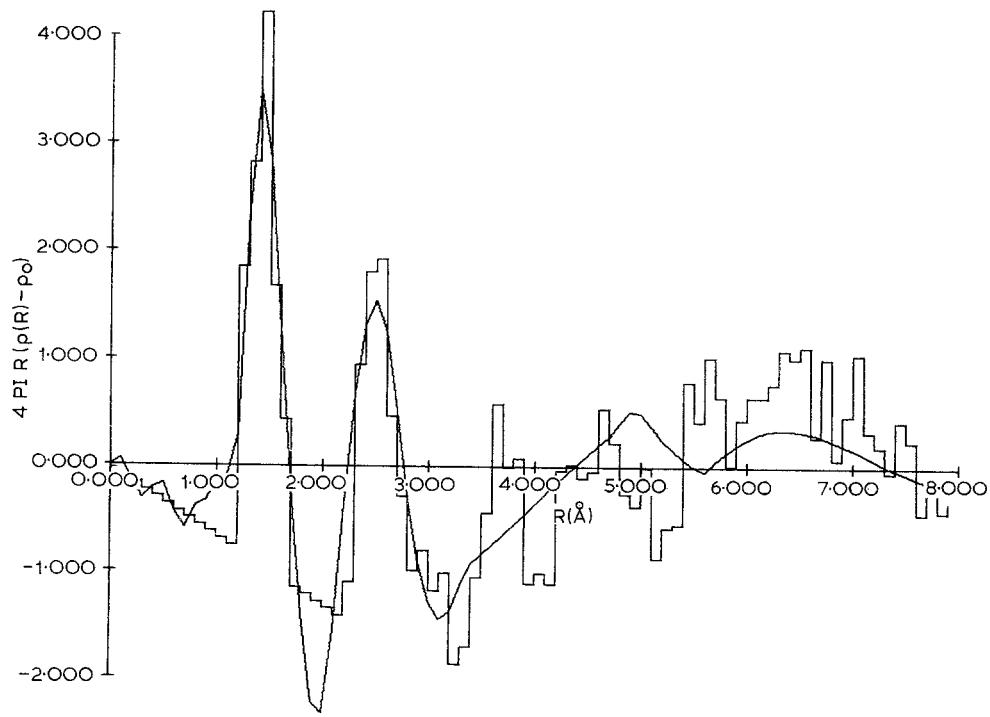

Figure 8 Observed $G(r)$ for annealed isotactic polystyrene superimposed on calculated $G(r)$ based on crystal structure as determined by Natta and Corradini [27].

involves nearly equal numbers of inter- and intramolecular contributions. The intramolecular spacings are almost all between phenyl atoms and chain atoms while the intermolecular spacings are all phenyl-phenyl spacings between neighbouring chains. The fourth peak in the $G(r)$ involves three times as many spacings as the third but the causes are very similar and they are closely divided between inter- and intramolecular spacings. Nearly all intermolecular spacings are phenyl-phenyl and almost all intramolecular spacings are phenyl-chain. A few phenyl-phenyl spacings in this peak extend to atoms in the second co-ordination ring of chains, while some of the phenyl-chain spacings are within the reference repeat unit. The third and fourth peaks taken together cover the range of 3.4 to 5.2Å and involve 164 spacings, of which eighty-six are interchain. All but ten of the interchain spacings are between phenyl atoms and all but twenty of the intrachain spacings are between phenyl and chain atoms. Several authors have reported a peak in this spacing range and Krimm [7] has assigned this peak to: (a) alternate phenyl groups on the same chain and, (b) to spacings between phenyl carbons on one chain and main chain atoms on a neighbouring chain. On the basis of the present model, only 7% of the spacings in this range are from alternate phenyl groups and 6% are phenyl-chain spacings in adjacent chains. The older assignments [7, 8] account for only 13% of the spacings in this range observed in our model. The assignment of this peak in the $G(r)$ to phenyl-phenyl interchain and phenyl-chain intrachain spacings accounts for 87% of the spacings. The assignments made by previous authors appear to be incorrect.

The fifth broad peak, from 5.2 to 8Å (the fourth in the experimental patterns) involves nearly 700 spacings, two-thirds of which are interchain. The separation of spacing types into phenyl-phenyl for interchain and phenyl-chain for intrachain present in the third and fourth peaks breaks down for the fifth peak. 70% of the phenyl-chain distances are interchain and 4% of the phenyl-phenyl distances are intrachain. This is caused largely by two features of the crystal structure: the c-axis repeat at 6.65Å and the interchain axis spacing of 7.3Å. The 6.65Å c repeat places phenyl rings directly above and below the reference atom, resulting in many intrachain phenyl-phenyl contributions to the fifth peak. The 7.3Å chain spacing places two chains in the proper interchain position for phenyl-chain spacings to occur. If only these two features are considered, half of the observed spacings are left unaccounted for.

There are numerous contributions to the scattering at separations beyond 8Å, most of which are intermolecular in origin.

6. Discussion and conclusions

This study poses one major question: why does the density of the sample increase when the long range spacings increase? A possible answer to this question is found in the structure of the molecule and repeat unit.

The phenyl ring predominates in the structure of a polystyrene repeat unit. It contains three-fourths of the mass of the repeat unit, and the distance across the phenyl ring to the chain is about twice as long as the contribution of the repeat unit to the length of the chain. The size of the phenyl rings prevents an isotactic polystyrene chain from adopting a planar zig-zag conformation (all chain atoms in the same plane) because this would produce too little separation between the phenyl rings. Spacings between phenyl rings are increased by rotations about chain bonds, resulting in a helix with three repeat units in each turn and 6.65Å between equivalent phenyls (Fig. 7). The phenyl rings can also act as "bumpers" and prevent the close approach of neighbouring molecules.

For the atactic material, containing a number of syndiotactic linkages, phenyl rings can be separated without the helix formation necessary in the isotactic molecule. Sections of molecule in planar zig-zag conformation, with phenyl rings in syndiotactic configuration, place all side groups "above" the chain (Fig. 9), allowing close approach of neighbouring chains. It is suggested by our study that the density of the atactic polymer is less than that of the isotactic because of the efficient intramolecular packing and long range order present in stereoregular polymers. Three experimental observations support this suggestion. Comparing RDFs for atactic and isotactic samples, we find for the isotactic: (a) an intensity decrease for the 5Å peak, and a shift to lower spacing, (b) an intensity increase and shift to higher spacings for the peak near 6Å, (c) an intensity decrease and shift to higher spacings for the 11Å peak. A sequence of syndiotactic linkages and a planar zig-zag conformation results in a repeated 5.2Å spacing (Fig. 9). Note that such a structure cannot occur in an isotactic macro-

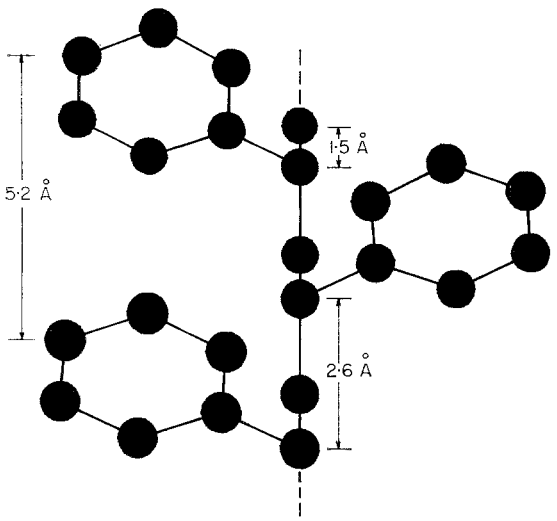

Figure 9 A syndiotactic sequence in atactic polystyrene.

molecule. Instead, the repeat units form a helix with a 6.65Å repeat distance, and the helical structure, with its phenyl rings protruding radially, can prevent the close approach of neighbouring molecules.

Much of the similarity between RDFs of different samples is caused by the large size of the phenyl ring, since the distribution of distances within a repeat unit is independent of the thermal history or tacticity of the sample, and includes distances as large as 6Å in polystyrene. This, however, does not explain all the observations as indicated above. An additional cause must be a similarity, at least at short range, between the structure of the different materials. We conclude that in all glassy polystyrene samples there is a tendency for phenyl groups to be sterically separated and for chain segments to pack parallel to each other; this supports the original suggestion by Kilian and Boueke [8] of the important role of steric hindrance in determining molecular conformation.

Acknowledgements

Support from an NDEA Traineeship to S. M. Wecker is gratefully acknowledged. Portions of this paper constituted an M.S. thesis submitted by this author in 1970 to Northwestern University. We wish to thank Dr F. L. Saunders of the Dow Chemical Company for providing the polystyrenes. Mr John Dhuey performed GPC measurements on the atactic samples in the Polymer Characterization Facility at Northwestern University. This research was supported by the Advanced Research Projects Agency through the Northwestern University Materials Research Center under Contract No. SD-67.

References

1. B. WUNDERLICH, D. M. BODILY, and M. H. KAPLAN, *J. Appl. Phys.* **35** (1964) 95.
2. R. F. BOYER, *Rubber Chem. & Technol.* **36** (1963) 1303.
3. A. J. KOVACS, *Fortschr. Hochpolym. -Forsch.* **3** (1963) 394.
4. J. R. KATZ, *Trans. Faraday Soc.* **32** (1936) 77.
5. G. L. SIMARD and B. E. WARREN, *J. Amer. Chem. Soc.* **58** (1936) 507.
6. A. BJØRNHAUG, Ø. ELLEFSEN, and B. A. TØNNESEN, *J. Polymer Sci.* **12** (1954) 621.
7. S. KRIMM, *J. Phys. Chem.* **57** (1953) 22.
8. H.-G. KILIAN and K. BOUEKE, *J. Polymer Sci.* **58** (1962) 311.
9. T. G. ROCHOW and E. G. ROCHOW, *J. Phys. Coll. Chem.* **55** (1951) 9.
10. T. G. F. SCHOON and O. TEICHMANN, *Kolloid-Z.* **197** (1964) 35.
11. G. S. Y. YEH and P. H. GEIL, *J. Macromol. Sci. (Phys.)* **B1** (1967) 235.
12. W. FRANK, H. GODDAR, and H. A. STUART, *J. Polymer Sci.* Part B, **5** (1967) 711.
13. S. H. CARR, P. H. GEIL, and E. BAER, *J. Macromol. Sci. (Phys.)* **B2** (1968) 13.
14. A. SIEGMANN and P. H. GEIL, *ibid* **B4** (1970) 239, 273.
15. R. E. ROBERTSON, *J. Phys. Chem.* **69** (1965) 1575.
16. L. H. SCHWARTZ, L. A. MORRISON, and J. B. COHEN, *Advances in X-ray Anaylsis* **7** (1963) 281.
17. M. E. MILBERG, *J. Appl. Phys.* **29** (1958) 64.
18. B. E. WARREN and R. L. MOZZI, *Acta Cryst.* **21** (1966) 459.
19. S. L. STRONG and R. KAPLOW, *ibid* **23** (1967) 38.
20. G. S. CARGILL, III, *J. Appl. Cryst.* **4** (1971) 277.
21. R. KAPLOW, S. L. STRONG, and B. L. AVERBACH, *Phys. Rev.* **138** (1965) A1336.
22. K. FURUKAWA, *Reports Prog. Phys.* **25** (1962) 395.
23. R. MCWEENY, *Acta Cryst.* **4** (1951) 513.
24. H. P. HANSON, F. HERMAN, J. D. LEA, and S. SKILLMAN, *ibid* **17** (1964) 1040.
25. D. T. KEATING and G. H. VINEYARD, *ibid* **9** (1956) 895.
26. A. H. COMPTON and S. K. ALLISON, "X-rays in Theory and Experiment", Second edition, (Van Nostrand, Princeton, New Jersey, 1935) p. 782.
27. G. NATTA and P. CORRADINI, *Makromol. Chemie* **16** (1955) 77.

Received 10 February and accepted 15 May 1972.